

# Distance distributions of photogenerated charge pairs in organic photovoltaic cells

Alex J. Barker, Kai Chen and Justin M. Hodgkiss\*

The MacDiarmid Institute for Advanced Materials and Nanotechnology, New Zealand.

School of Chemical and Physical Sciences, Victoria University of Wellington, New Zealand.

\* E-mail: Justin.Hodgkiss@vuw.ac.nz

## Contents

<b>1. Sample Preparation .....</b>	<b>1</b>
<b>2. Broadband visible TA spectra .....</b>	<b>2</b>
<b>3. Broadband infrared TA spectra .....</b>	<b>3</b>
<b>4. Comparison with devices prepared in inert atmosphere .....</b>	<b>4</b>
<b>5. Polarization anisotropy decay at 290 K and 10 K.....</b>	<b>5</b>
<b>6. Early MEH-PPV:PCBM recombination.....</b>	<b>6</b>
<b>7. Fitting free charge yields using density-dependent kinetic model.....</b>	<b>7</b>
<b>8. Rate distribution fits from 10 K recombination; bimodality of recombination rate distributions.....</b>	<b>10</b>
<b>9. References .....</b>	<b>16</b>

## 1. Sample Preparation

All materials were commercially sourced, from the following suppliers:

- PC<sub>61</sub>BM – Aldrich.
- P3HT – Aldrich. Average MW 30 – 60 kDa
- PCDTBT – Solaris Chem Inc. Typical MW 20 – 45 kDa
- PCPDTBT – Solaris Chem Inc. Typical MW 15 – 25 kDa
- MEH-PPV – American Dye Source, Inc. MW > 100 kDa

Samples were spin-coated onto spectroil fused silica substrates in air and at room temperature before being transferred into a vacuum cryostat for measurements. The substrates were cleaned prior to coating by sonication in acetone and then in isopropanol. Each sample was prepared from solution as follows:

- P3HT:PC<sub>61</sub>BM (1:1, and 19:1), 30 mg/mL total concentration in 1,2-dichlorobenzene. Spin coated at 2000 RPM. Where indicated, the film was annealed by exposure to a solvent (1,2-dichlorobenzene) vapor saturated atmosphere at room temperature for 30 minutes.<sup>1</sup>
- PCPDTBT:PC<sub>61</sub>BM (1:2), 30 mg/mL total concentration in chlorobenzene, with 5% 1,8-octanedithiol.<sup>2</sup> Spin coated at 1200 RPM.
- PCDTBT:PC<sub>61</sub>BM (1:4), 30 mg/mL total concentration in 1,2-dichlorobenzene. Spin coated at 1500 RPM.
- PCDTBT:PC<sub>61</sub>BM (19:1), 7 mg/mL total concentration in 1,2-dichlorobenzene. Spin coated at 2000 RPM.

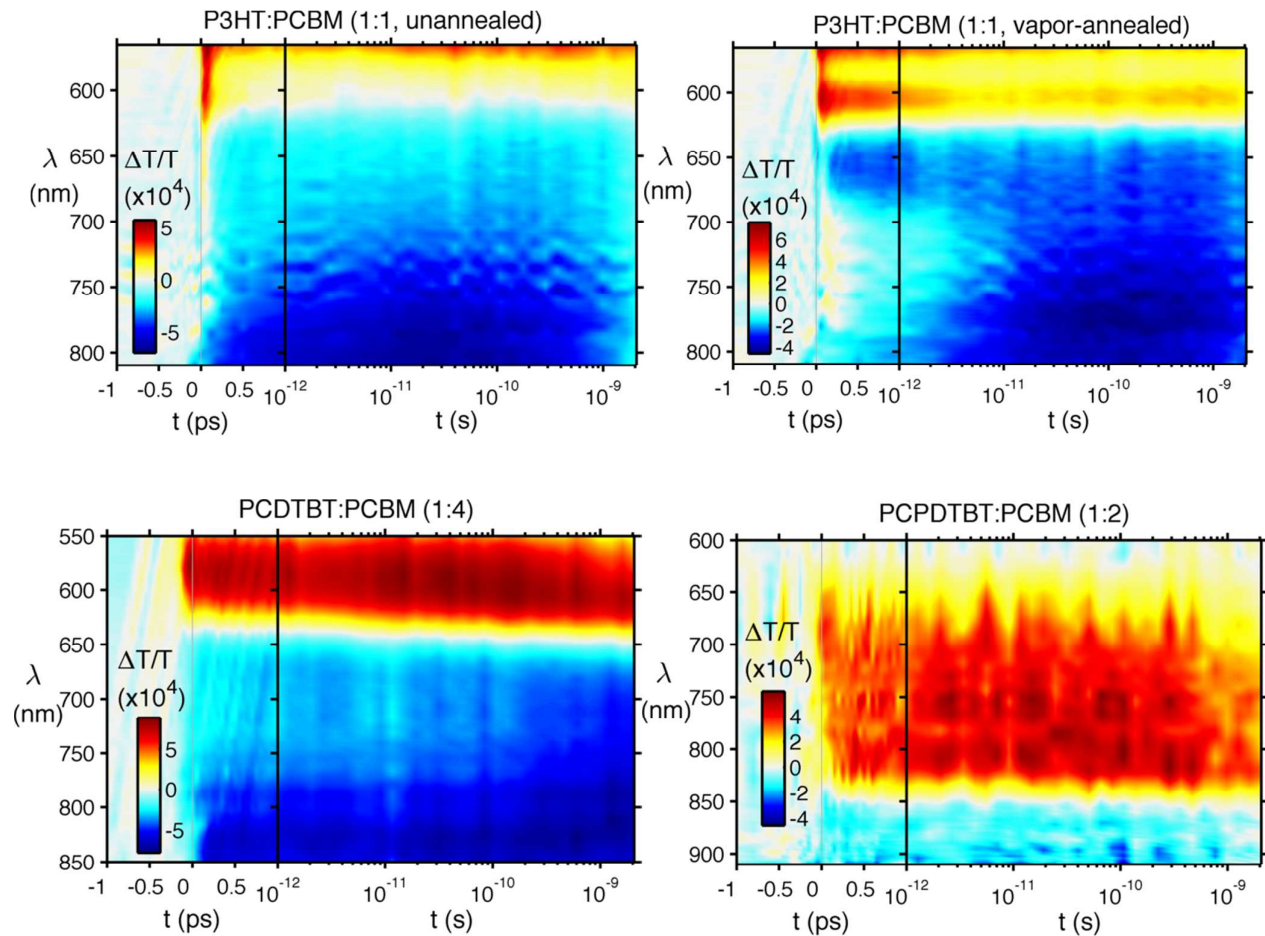
- MEH-PPV:PC<sub>61</sub>BM (1:1), 15 mg/mL total concentration in chlorobenzene. Spin coated at 1700 RPM.
- MEH-PPV:PC<sub>61</sub>BM (1:4), 15 mg/mL total concentration in chlorobenzene. Spin coated at 1200 RPM.

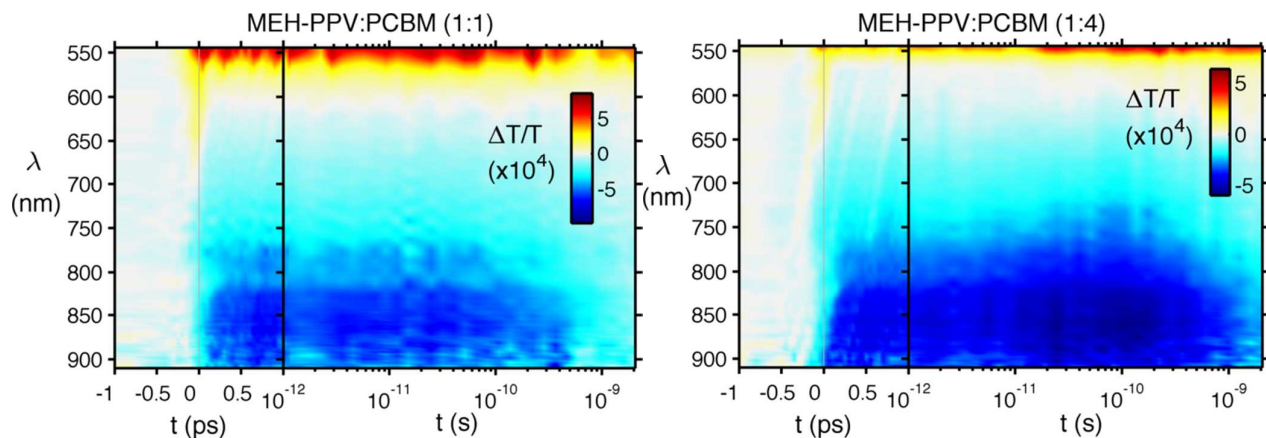
In order to verify that brief exposure to air during sample preparation was not a problem, we also prepared an annealed P3HT:PCBM under inert conditions, as described in section 4.

## 2. Broadband visible TA spectra

Ultrafast broadband transient absorption spectra of the samples were collected using an amplified broadband probe source (NOPA, reference 3) and 100 fs excitation at 532 nm, generated in a parametric amplifier (TOPAS). As with the anisotropy measurements, pump-probe delay was varied using a retroreflector mounted on a mechanically controlled delay stage. The probe light was dispersed, collected and read-out at 3 kHz using the spectrometer and photodiode array described in the main text.

The TA maps shown below were taken at room temperature, and low excitation density (at or below  $\sim 10 \mu\text{J}/\text{cm}^2$ ) to avoid artifacts from higher order processes such as exciton-exciton and exciton-charge annihilation. Nearly all samples show a broad, long-lived photoinduced absorption at 800 nm (the probing wavelength for the tunneling and intensity-dependent recombination measurements). The only exception is PCPDTBT:PCBM, for which 800 nm is coincident with the GSB.

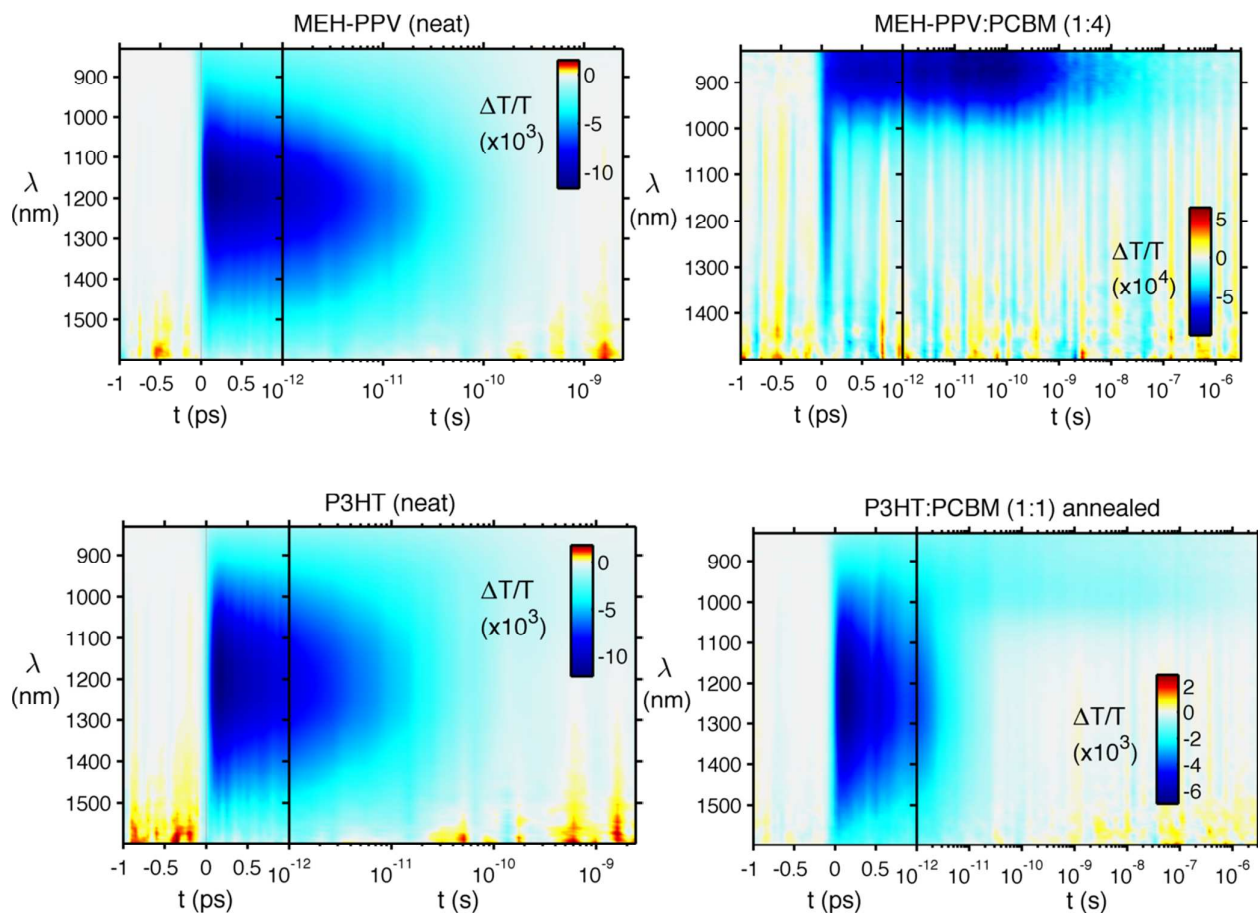


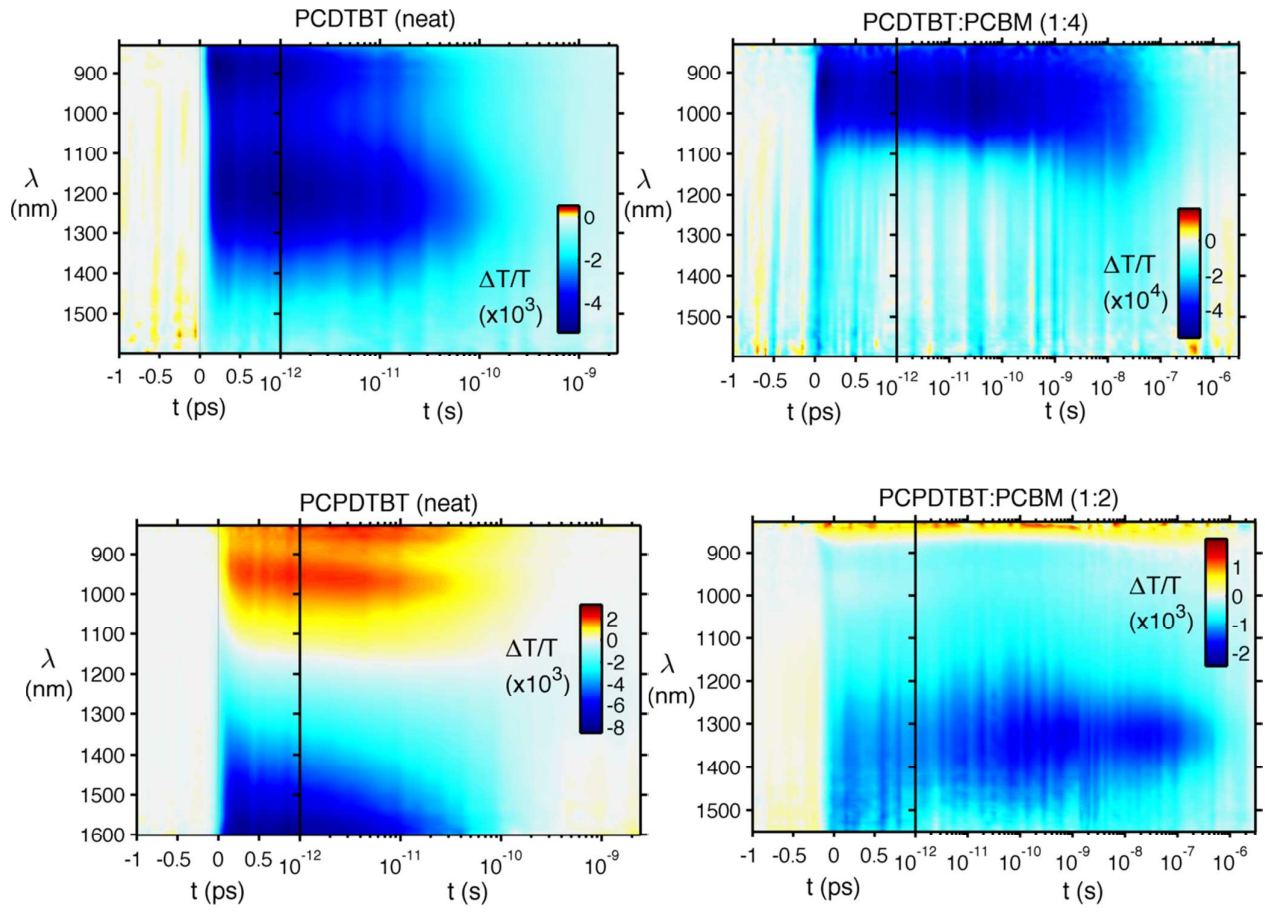


### 3. Broadband infrared TA spectra

For the following TA maps were collected using an unamplified broadband IR probe generated by focusing 800 nm pulses in to a YAG crystal, with detection *via* an InGaAs linear photodiode array. Data up to time delays of 1 ns was collected using 100 fs, 532 nm pump pulses from the TOPAS. For data at time delays greater than 1 ns, the pump was the electronically delayed 2<sup>nd</sup> harmonic of our Q-switched Nd:YVO<sub>4</sub> laser as described in the main text. In all cases, excitation density was approximately 10  $\mu\text{J}/\text{cm}^2$ .

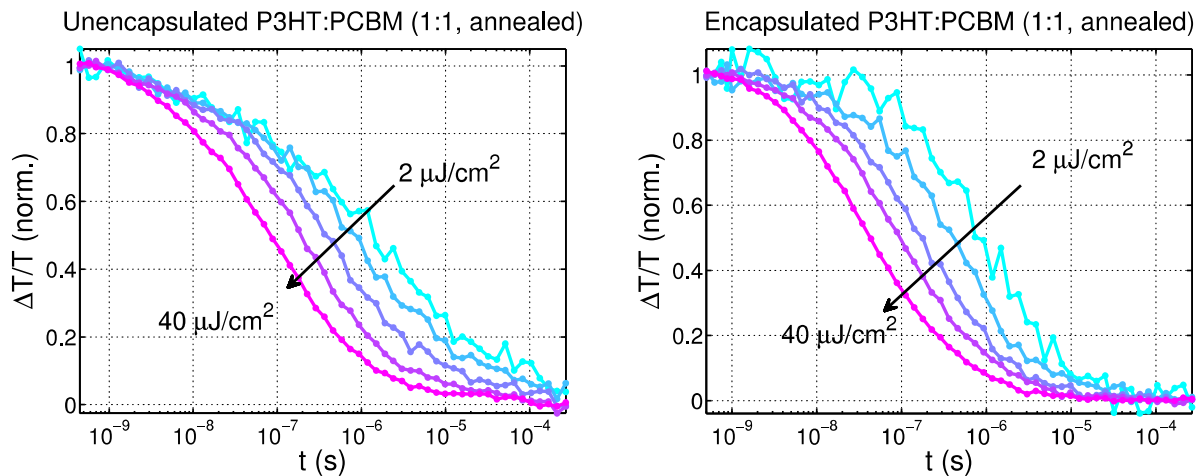
For all of the blends studied here, the addition of PCBM results in distinct changes from the neat spectra, allowing us to clearly distinguish the spectral signatures of excitons and charges. Furthermore, we can confirm that in all blends, only charges are present on the ns- $\mu\text{s}$  timescales relevant to the recombination measurements in the main text.





#### 4. Comparison with devices prepared in inert atmosphere

The unencapsulated sample refers to the annealed blend used throughout this article, prepared in ambient conditions (but placed in a vacuum cell during spectroscopy). The encapsulated sample was prepared in a nitrogen-filled glovebox, thermally annealed at 160 °C for 10 minutes, and encapsulated under epoxy and a glass slide before being removed from the glovebox for spectroscopy.





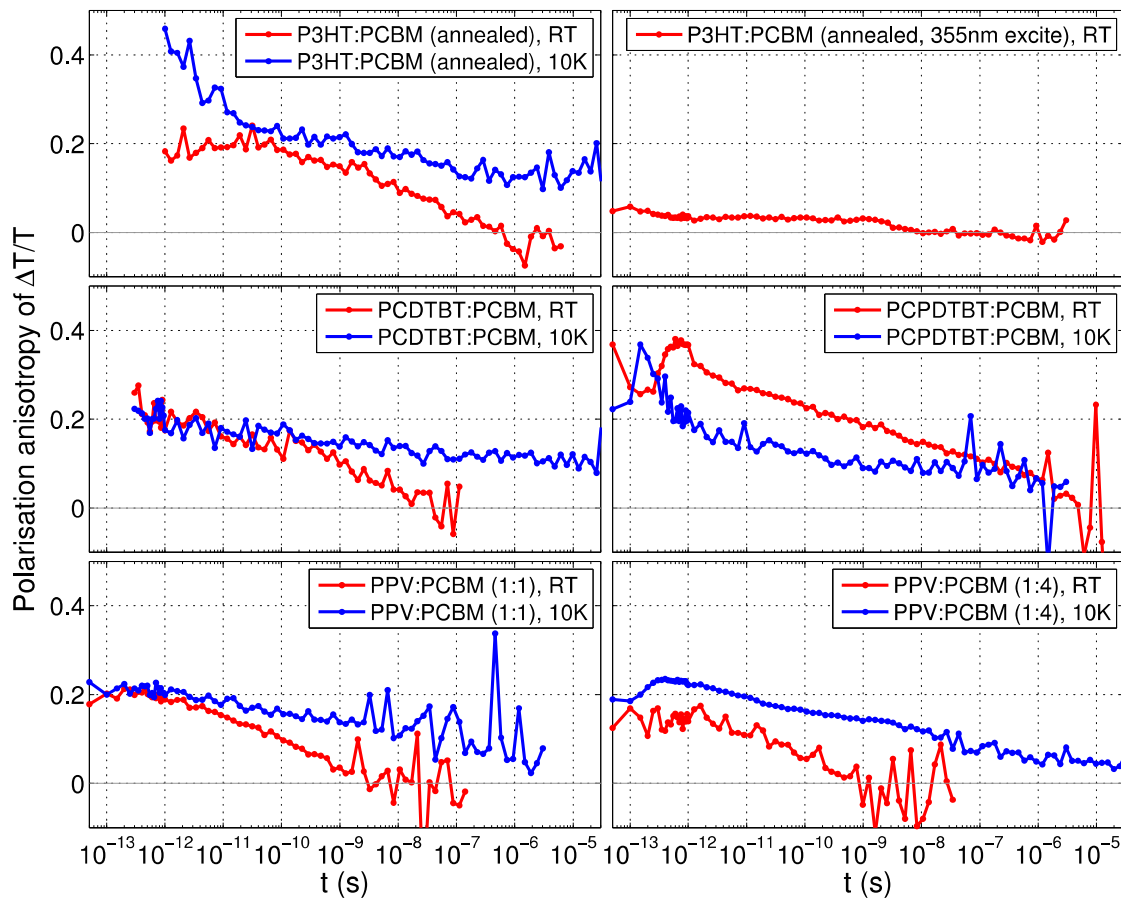
## 5. Polarization anisotropy decay at 290 K and 10 K

Polarization anisotropy decay of the transient absorption signal was measured by inserting a polarizing beamsplitter into the path of the probe pulse after interaction with the sample, splitting the light into components parallel ( $\parallel$ ) and perpendicular ( $\perp$ ) to the excitation pulse. By simultaneously measuring the transient absorption of these components on separate channels, the time- and wavelength-dependent polarization anisotropy  $r(\frac{\Delta T}{T})$  was given by:

$$r(\frac{\Delta T}{T}) = \frac{(\frac{\Delta T}{T})_{\parallel} - (\frac{\Delta T}{T})_{\perp}}{(\frac{\Delta T}{T})_{\parallel} + 2(\frac{\Delta T}{T})_{\perp}}.$$

A non-zero polarization anisotropy indicates some net alignment of the absorption dipoles of the excited states with respect to the excitation pulse (with a maximum possible value of 0.4 for a population of perfectly aligned dipoles with respect to the excitation pulse polarization).

The figure below shows anisotropy probed at 800 nm, after excitation at 532 nm. For time delay greater than 2 ns, the excitation light was generated as described in the main body of this article. For times less than 2 ns, 100 fs excitation pulses were generated in an optical parametric amplifier (TOPAS) with pump-probe delay varied using a mechanically controlled delay stage.



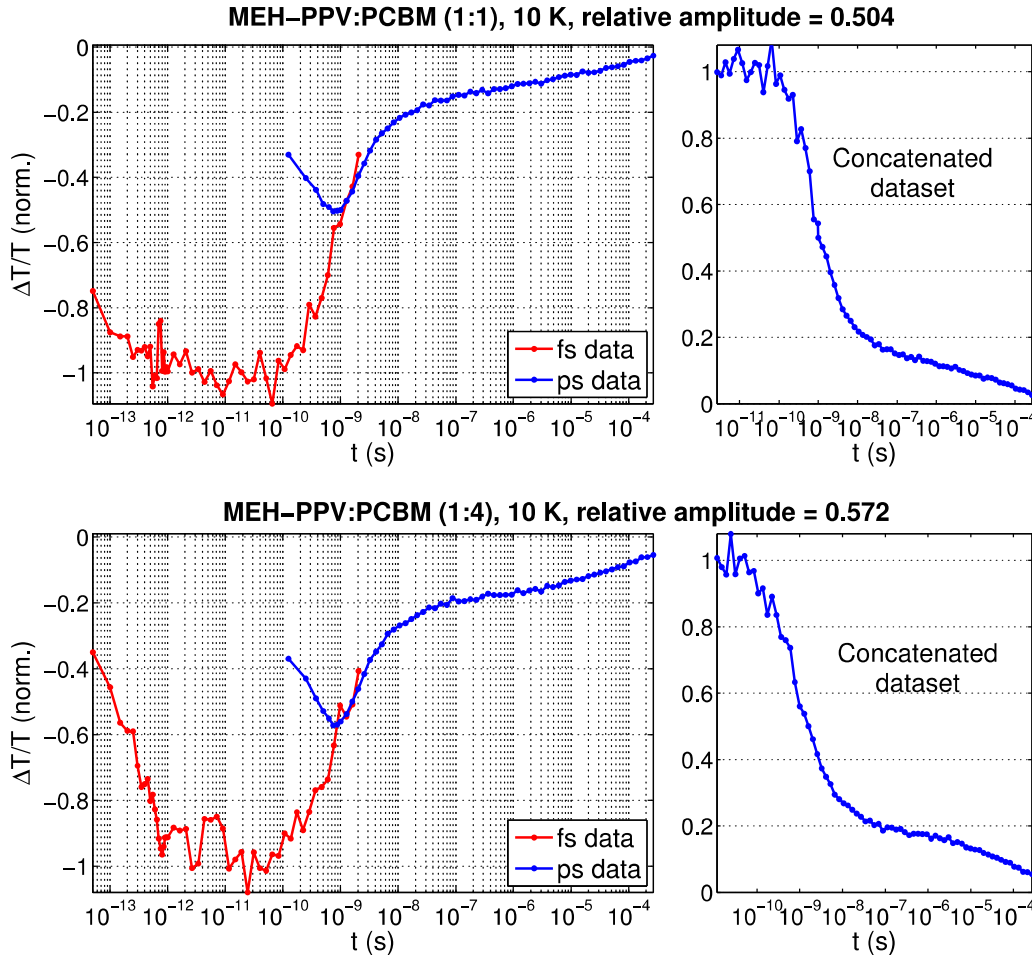
Nearly all materials show drastically reduced anisotropy decay at 10 K, due to charges becoming immobile at sufficiently low temperature. The only exception is PCPDTBT:PCBM, which may reflect the fact that we probed the ground-state bleach (GSB) in that case, which contains contributions from all excitations.

Interestingly, in P3HT:PCBM anisotropy is almost completely absent when the sample is excited at 355 nm, a wavelength at which excited states are preferentially generated on the PCBM molecule. Since the 800 nm probe is only sensitive to cationic absorption within the polymer, we can conclude that no memory of dipole orientation is retained in photogenerated holes from the initial excitation in PCBM.

## 6. Early MEH-PPV:PCBM recombination

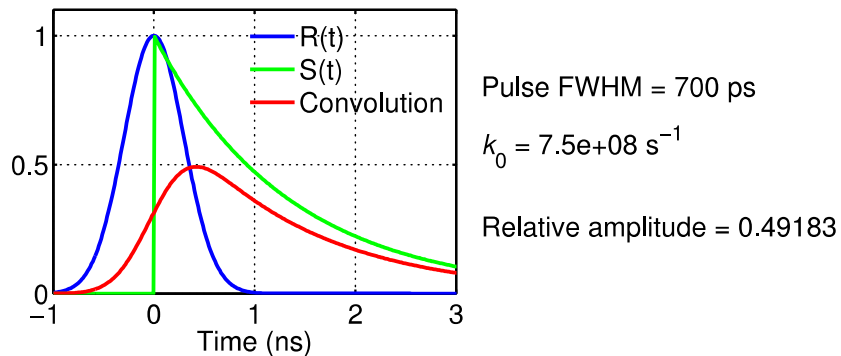
An appreciable fraction of photogenerated charge pairs within MEH-PPV:PCBM blends undergo recombination in less than 1 ns, faster than the time resolution of our TA experiment when using the electronically delayed excitation source. Additional data was therefore collected using a 100 fs excitation pulse and mechanical delay stage, capable of collecting data up to a delay of several nanoseconds. Data from the two time ranges was normalized so as to coincide from 1 – 2 ns.

The combined datasets are shown below. Also shown is the relative amplitude of the fs and ps peaks, which is used to correct the free charge fraction fitted from intensity-dependent recombination measurements (see following section).



The collected data represents the convolution of our instrument response function  $R(t)$  and the true signal decay,  $S(t)$ . This convolution is given by  $I(t) = \int R(t - t')S(t)dt'$ .

If we take  $R(t)$  as a Gaussian pulse with FWHM = 700 ps, and  $S(t)$  as a monoexponential with rate =  $7.5 \times 10^8 \text{ s}^{-1}$ , a simple numerical calculation of the convolution function predicts a relative amplitude of 0.49, in agreement with the concatenated datasets shown above.



## 7. Fitting free charge yields using density-dependent kinetic model

The figures below show fits to the intensity-dependent TA data, from which figure 5 in the main text was compiled.

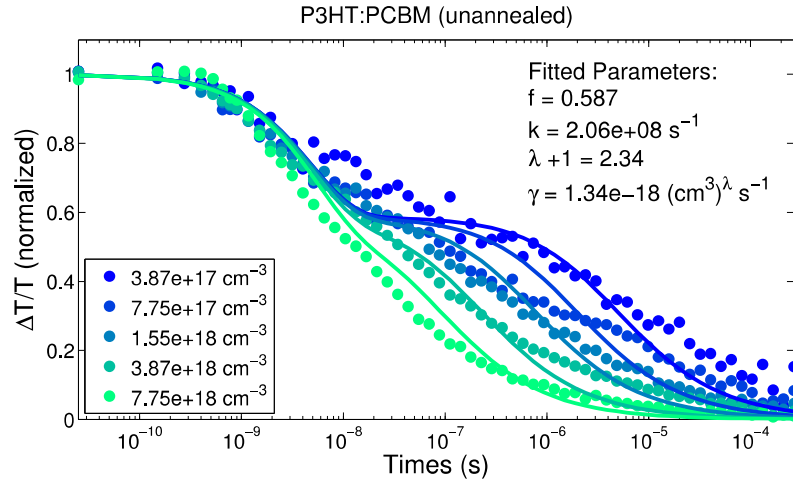
The data was collected at room temperature using an 800 nm probe, as described in the experimental details of the main text. The experiment allows us to track charge recombination from ns-μs timescales, and to investigate the dependence of charge recombination on charge density by repeating the measurement at a range of excitation intensities. We then apply the kinetic model described in Reference 4, which assumes a mechanism by which electron-hole pairs generated from exciton quenching rapidly thermalize to form either spatially separated ‘free’ charge pairs, or bound charge-transfer states, which tend to recombine *via* nongeminate and geminate recombination, respectively.

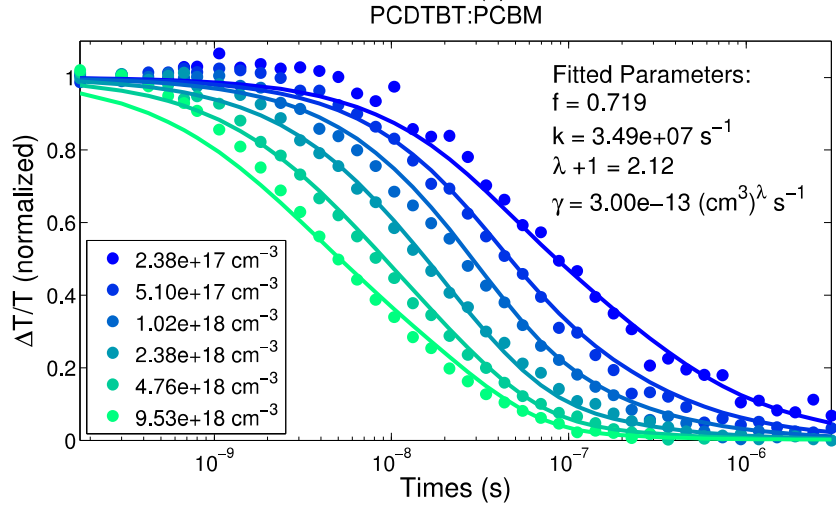
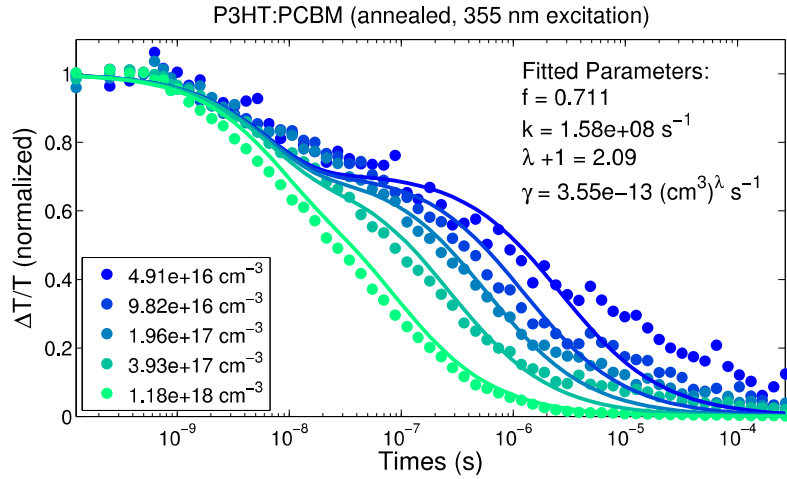
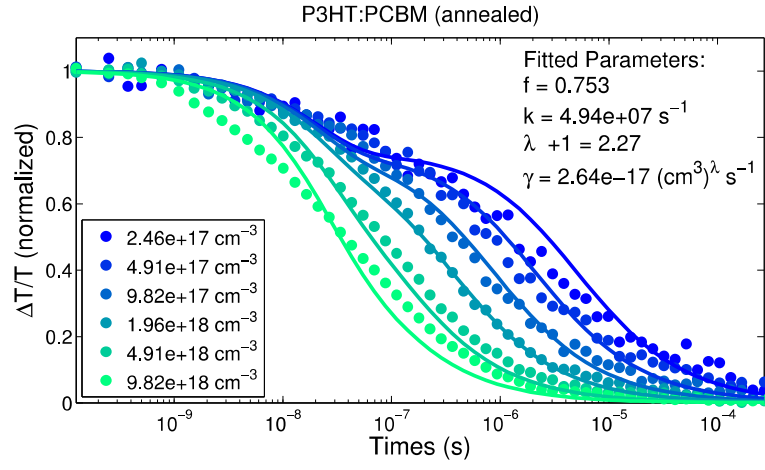
The model takes total charge density,  $N_0$ , as an initial condition for each curve (as the rate of charge photogeneration is significantly faster than the time resolution of this experiment) and applies a global fit to determine the relative contribution of geminate and non-geminate recombination – and by extension the relative proportion of free and bound charge pairs – within each sample. It turns out the rate equations for such a system can be solved, with the solutions for the time dependent populations in each state given by:

$$\begin{aligned} \text{CT}(t) &= N_0(1 - \Phi_{\text{free}}) \exp(-k_{\text{CT} \rightarrow \text{GS}}t) \\ \text{SSC}(t) &= (\lambda\gamma t + (\Phi_{\text{free}}N_0)^{-\lambda})^{-1/\lambda} \\ \text{GS}(t) &= N_0(1 - \Phi_{\text{free}})(1 - \exp(-k_{\text{CT} \rightarrow \text{GS}}t)) + \\ &\quad N_0\Phi_{\text{free}} - ((\lambda\gamma t + (\Phi_{\text{free}}N_0)^{-\lambda})^{-1/\lambda}), \end{aligned}$$

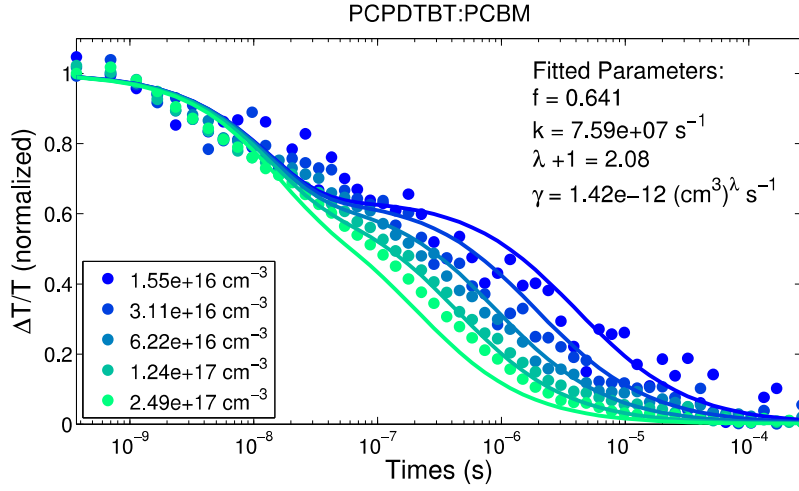
Where CT is the (bound) charge-transfer state population, SSC is spatially separated (‘free charge’) population (counting holes only), and GS is the population that has relaxed back to the ground state. The remaining parameters are left free to be globally fitted to the set of decay curves:  $\gamma$  the density-dependent recombination rate constant,  $\lambda + 1$  the order of the non-geminate recombination,  $k_{\text{CT} \rightarrow \text{GS}}$  the rate of geminate recombination, and  $\Phi_{\text{free}}$ , the fraction of free charges from the initial branching event.

Sample film thickness was measured by Dektak profilometer and optical density determined by UV-vis spectroscopy. These values were used along with the fluence (photons per square centimetre per pulse) of the excitation pulse to calculate the initial density of photogenerated charges for each dataset (shown in figure insets). Fitted parameters are shown for each sample (note: the fitted parameter  $f$  is the fraction of nongeminate recombination, presented as  $\Phi_{\text{free}}$  in the main text).



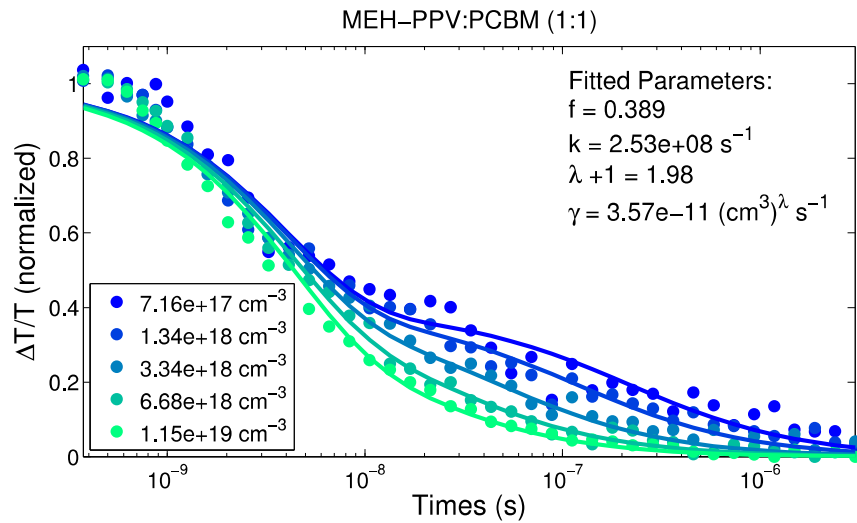
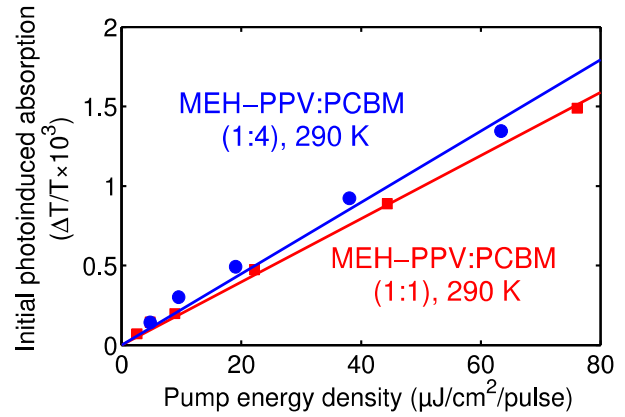




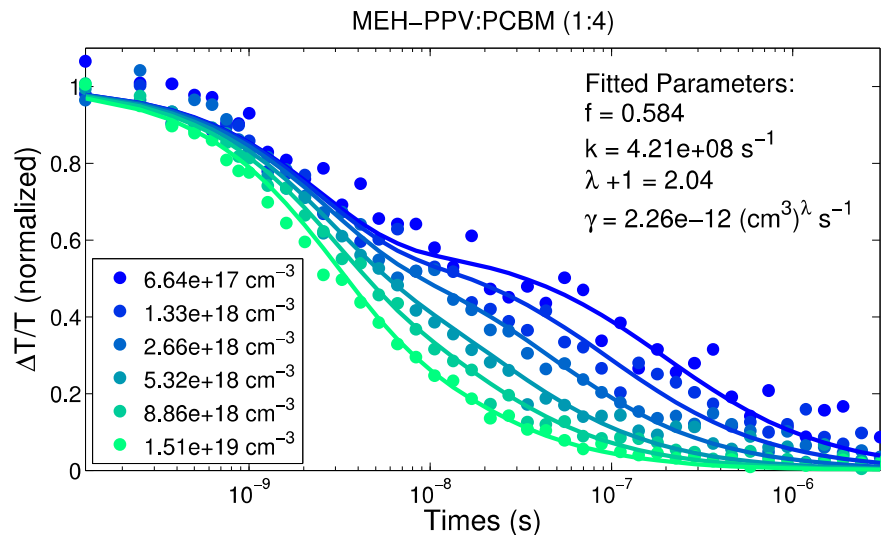


As described in SI section 4, MEH-PPV:PCBM blends exhibit appreciable recombination within the time resolution of this experiment. The fraction of subnanosecond recombination was quantified as (1 - 0.504) and (1 - 0.572) for the 1:1 and 1:4 blends respectively.

For both 1:1 And 1:4 blends of MEH-PPV:PCBM, the magnitude of the initial photoinduced absorption signal is close to linear with respect to the initial pump intensity. This indicates that negligible bimolecular recombination takes place within the convolution period, allowing us to attribute the ‘missing’ signal entirely to bound charge pairs, and apply a correction to  $\Phi_{\text{free}}$ , the yield of free charge pairs.



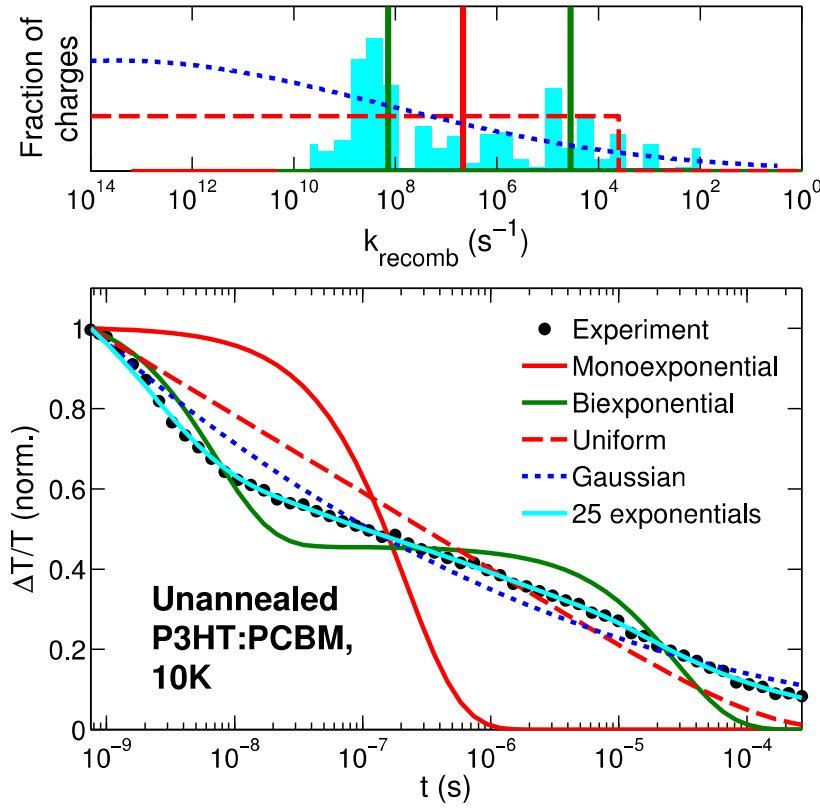
Undetected bound charge fraction = 1 - 0.504 = 0.496  
 □ Corrected free charge fraction =  $0.389/(1+0.496) = \mathbf{0.260}$



Undetected bound charge fraction =  $1 - 0.572 = 0.428$   
Corrected free charge fraction =  $0.584 / (1 + 0.428) = \mathbf{0.408}$

## 8. Rate distribution fits from 10 K recombination; bimodality of recombination rate distributions

By observing how closely simple distributions of rate constants fit the experimental decay for unannealed P3HT:PCBM at 10 K (below), we are guided towards a model that captures the data with minimal free parameters. The charge recombination dynamics appear to be described by a rapid early ( $< 10 \text{ ns}$ ) phase that may be fit by a narrow distribution of rate constants, followed by slower dynamics that clearly demand a much broader distribution of rate constants. A uniform series of logarithmically distributed rate constants with fixed equal amplitude predicts a decay that captures the overall dispersion, but fails to capture the apparent faster (CT) decay phase. A broad Gaussian distribution of rate constants leads to a slight improvement, however, failure to account for the transition between a fast and slower recombination leads to suggest that a bimodal distribution of rate constants is needed. A series of logarithmically distributed rate constants with independent amplitudes fits the data well, but the excess parameters impair quantitative comparison between samples. It can be seen that a bimodal rate distribution emerges after initialization with a flat distribution. Balancing the requirements to fit a bimodal rate distribution with minimal free parameters led us to fit to a rate distribution reflecting a double Gaussian charge pair distance distribution (i.e., double Gaussian on a logarithmic rate scale).



Full plots and fitted parameters for the data shown for all samples in figure 4 of the main text are shown below (left side). The double Gaussian distribution was defined as follows,

$$CT(k) = \exp \left[ -4 \ln(2) \left( \frac{-\ln\left(\frac{k}{k_{CT}}\right)}{k_{CT,FWHM}} \right)^2 \right], \text{ normalized to have area under curve (on a log scale)} = (1 - \Phi_{SC}),$$

$$SC(k) = \exp \left[ -4 \ln(2) \left( \frac{-\ln\left(\frac{k}{k_{CT}}\right) + \ln\left(\frac{k_{SC}}{k_{CT}}\right)}{k_{SC,FWHM}} \right)^2 \right], \text{ normalized to have area under curve (on a log scale)} = \Phi_{SC},$$

$$\text{Total fraction of charges}(k) = CT(k) + SC(k).$$

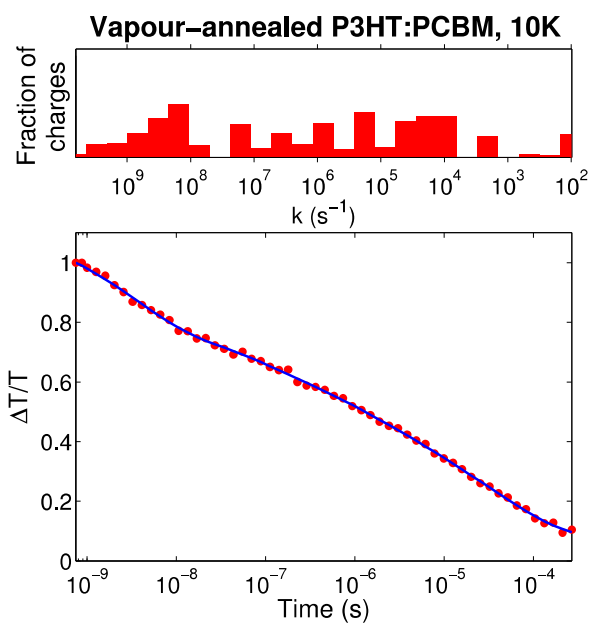
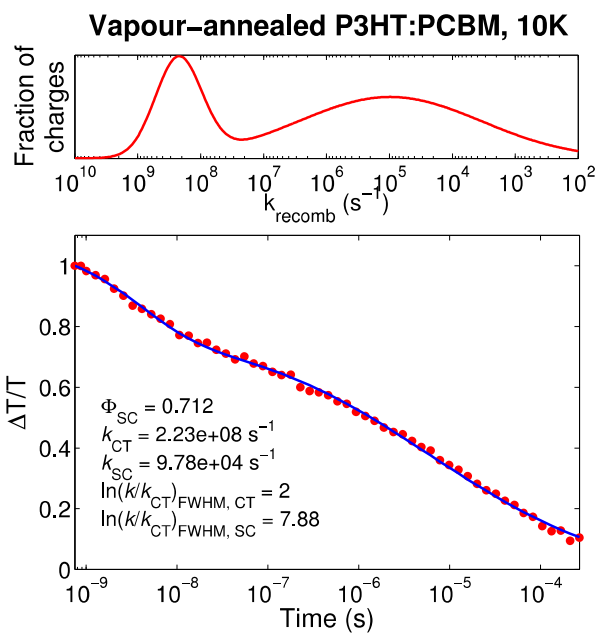
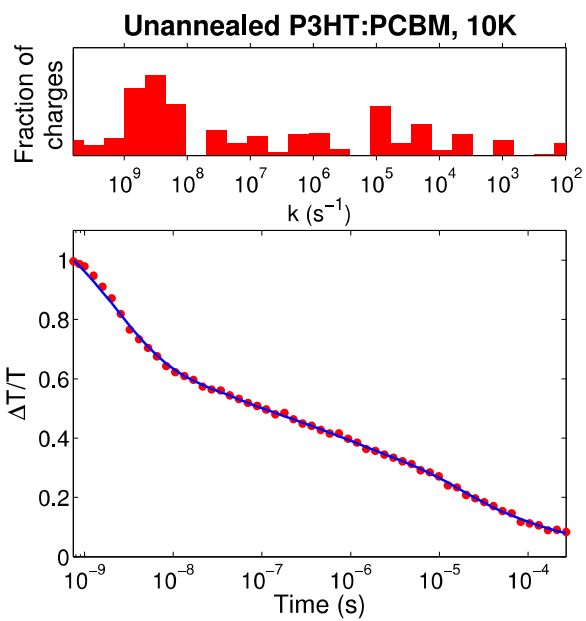
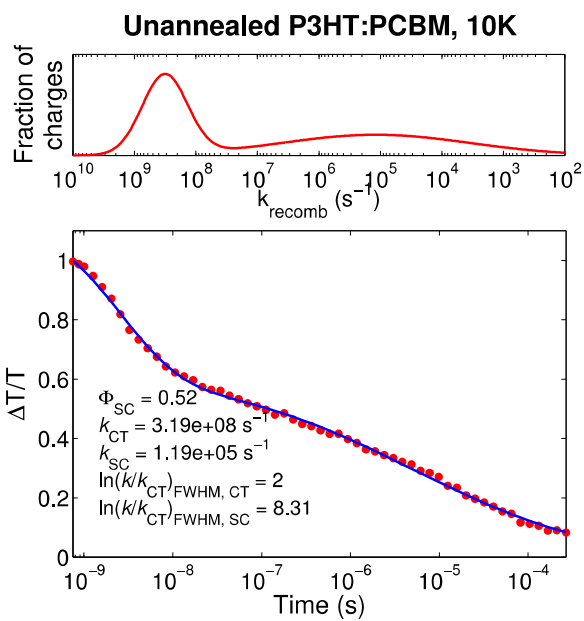
Where  $\Phi_{SC}$  is fraction of SCs,  $k$  is recombination rate,  $k_{CT}$  and  $k_{SC}$  are peak rate for CTs and SCs respectively, and  $k_{CT,FWHM}$  and  $k_{SC,FWHM}$  are the width of the distributions of CTs and SCs, respectively. The width of the bound charge pair distribution ( $k_{CT,FWHM}$ ) was fixed = 2, leaving four fitting parameters:  $\Phi_{SC}$ ,  $k_{CT}$ ,  $k_{SC}$ , and  $k_{SC,FWHM}$ .

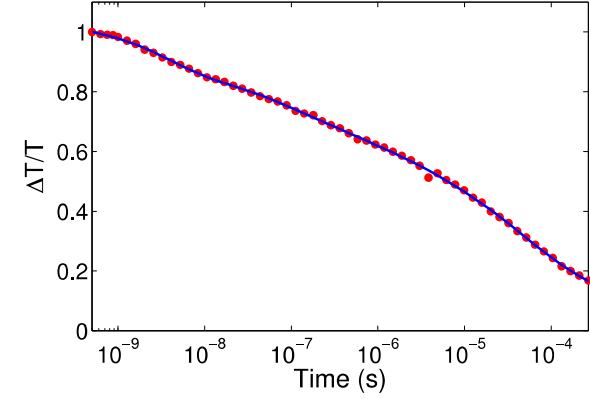
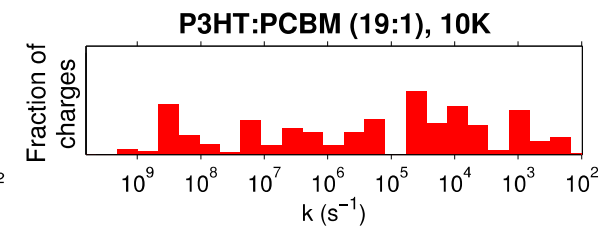
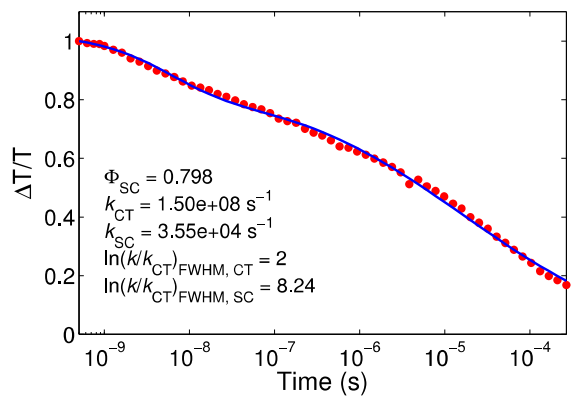
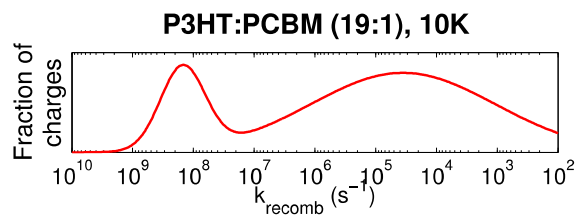
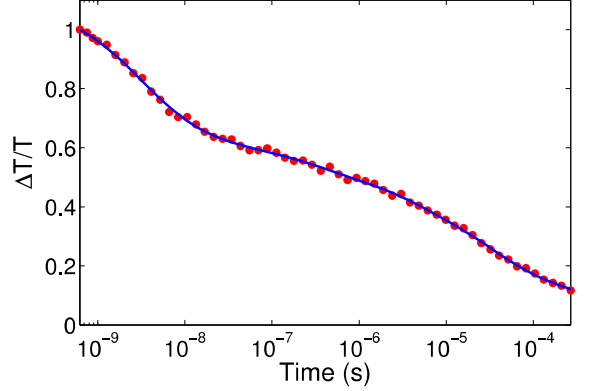
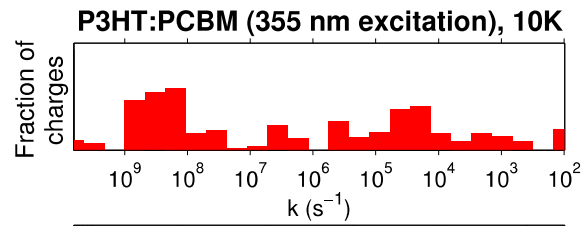
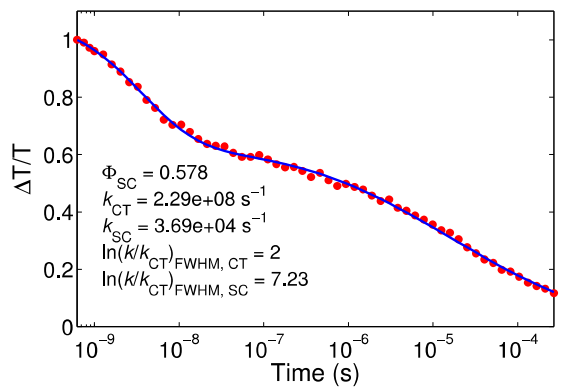
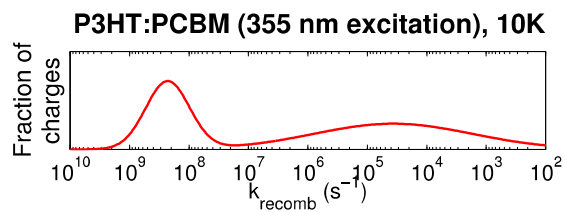
The fitting routine proved to be exceptionally robust, with the same fitted parameters being returned for a wide range of initial conditions. Fits for all materials were calculated from identical initial conditions.

While the bimodal Gaussian distribution generates time-dependent recombination in excellent agreement with experiment, it is not a unique solution. One alternative identified above is to define an ensemble of independent charge-pair populations, each with a well-defined monoexponential decay rate. Compared to the double-Gaussian fits, this approach is poorly parameterized and does not lend itself to physical interpretation. However, it has the advantage of being without bias in the distribution of rates (i.e. it does not presume a bimodal distribution).

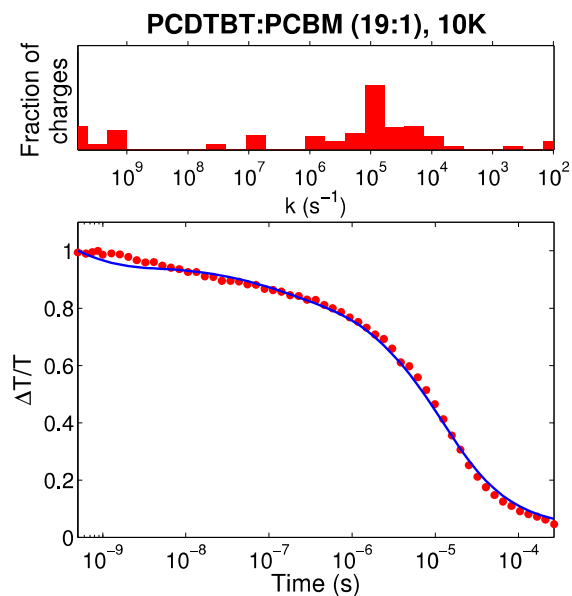
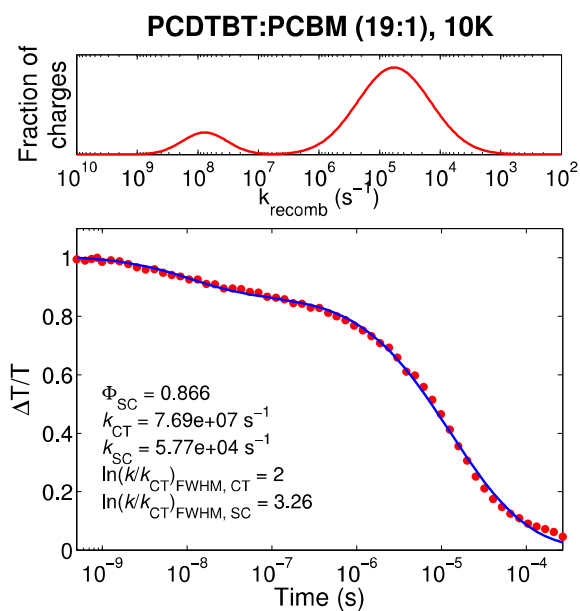
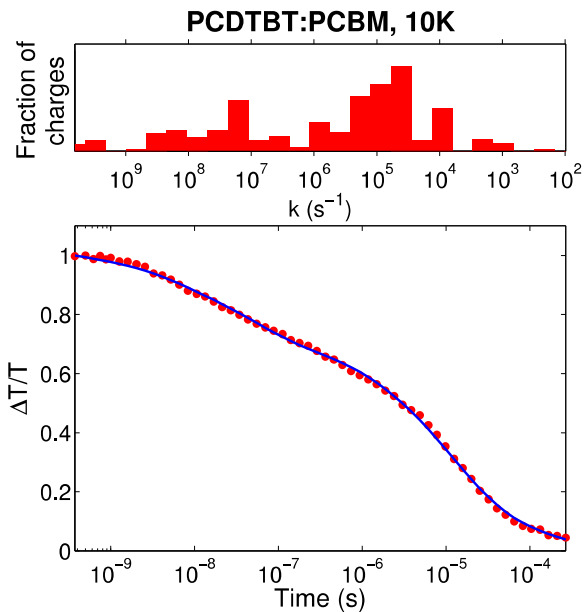
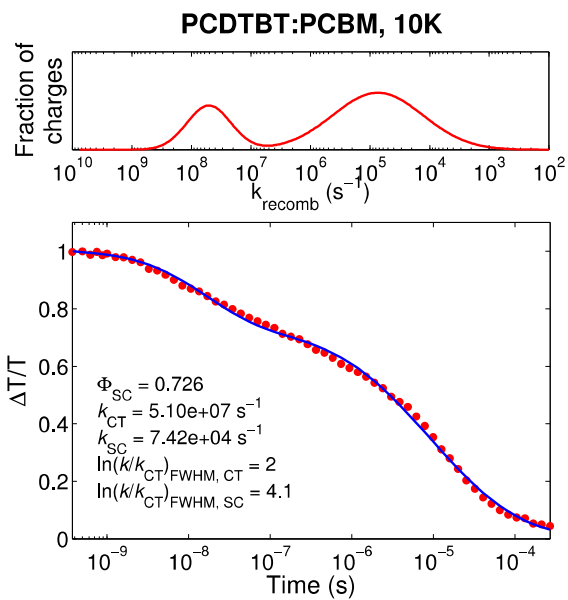
The fits shown below (right side) feature 25 rates logarithmically spaced from  $\sim 10^{10}$  to  $10^2 \text{ s}^{-1}$ . The fitted parameters are the 25 initial populations for each rate, with the initial condition being an equal distribution of charges across all rates.

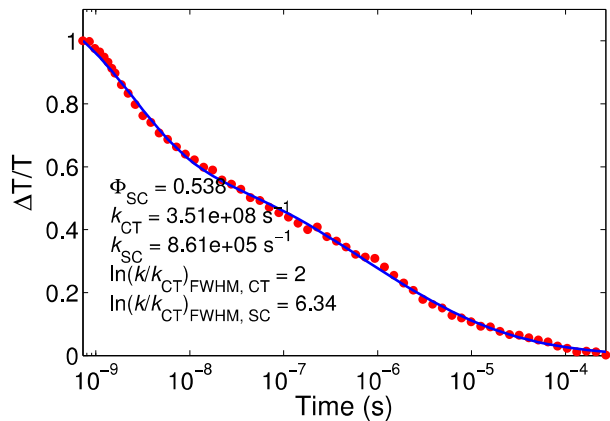
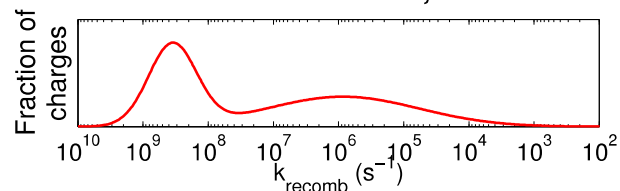
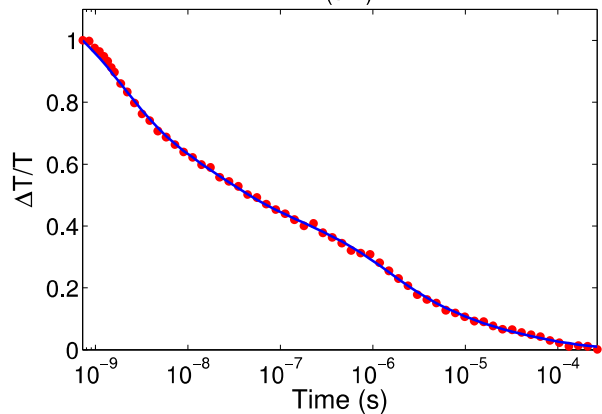
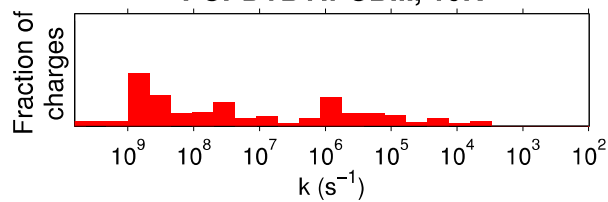
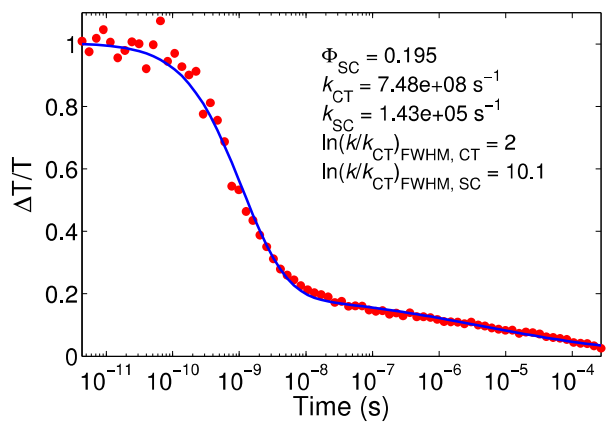
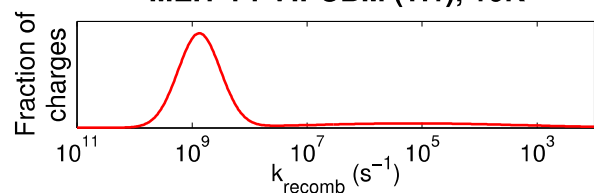
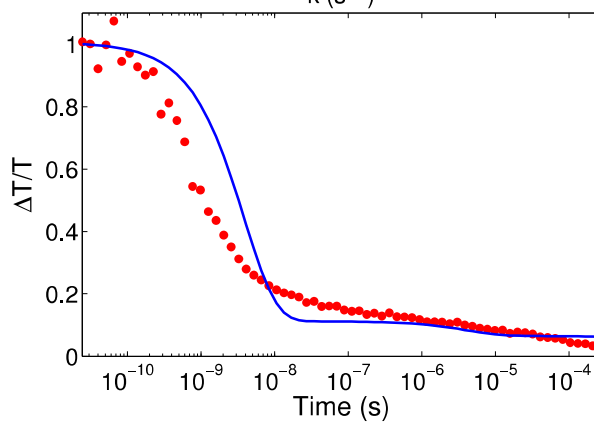
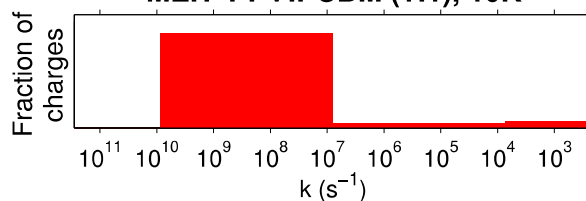
While the approach is not always successful, in most cases we see the emergence of a (somewhat noisy) bimodal distribution with an interpeak minima near  $10^7 \text{ s}^{-1}$  and a population distribution resembling those given by the double Gaussian fits.

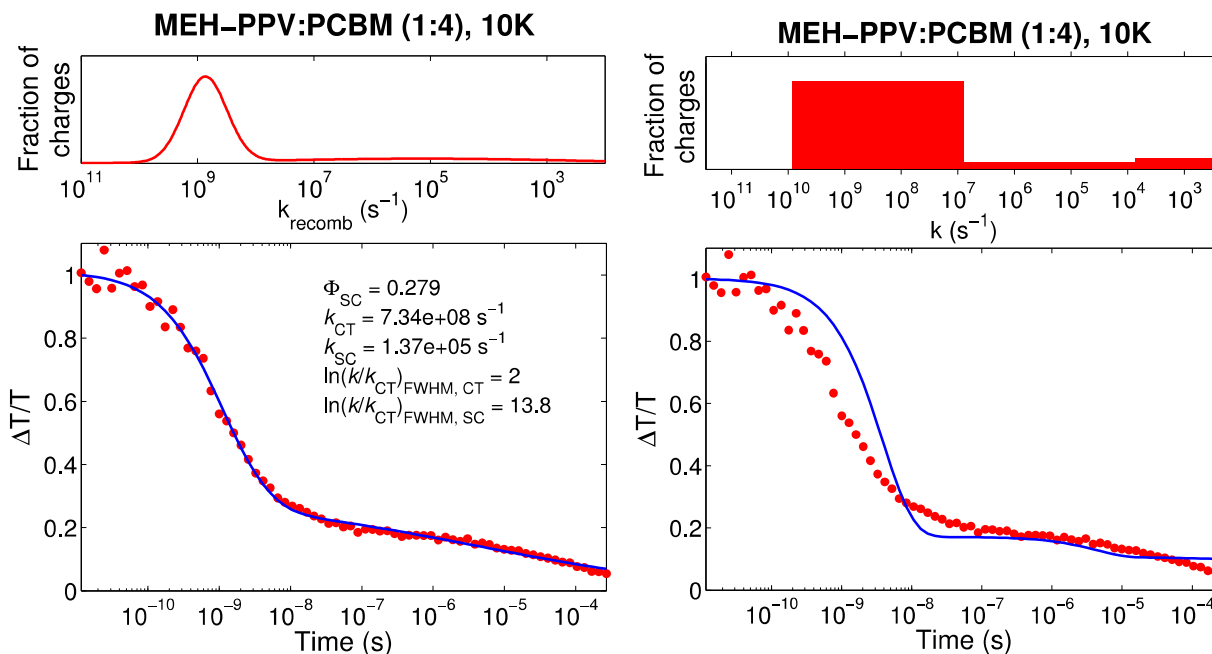








**PCPDTBT:PCBM, 10K****PCPDTBT:PCBM, 10K****MEH-PPV:PCBM (1:1), 10K****MEH-PPV:PCBM (1:1), 10K**



## 9. References

- (1) Zhao, Y.; Xie, Z.; Qu, Y.; Geng, Y.; Wang, L. *Appl. Phys. Lett.* **2007**, *90*, 043504.
- (2) Etzold, F.; Howard, I. a; Forler, N.; Cho, D. M.; Meister, M.; Mangold, H.; Shu, J.; Hansen, M. R.; Müllen, K.; Laquai, F. *J. Am. Chem. Soc.* **2012**, *134*, 10569.
- (3) Manzoni, C.; Polli, D.; Cerullo, G. *Rev. Sci. Instrum.* **2006**, *77*, 023103.
- (4) Howard, I. A.; Mauer, R.; Meister, M.; Laquai, F. *J. Am. Chem. Soc.* **2010**, *132*, 14866.